Polymer 49 (2008) 5072–5083

Contents lists available at ScienceDirect

Polymer

journal homepage: www.elsevier.com/locate/polymer

Structural study of a series of ethylene–tetrafluoroethylene copolymers with various ethylene contents, Part 2: Phase transition behavior investigated by temperature dependent measurements of X-ray fiber diagrams

Suttinun Phongtamrug [a], Kohji Tashiro [a,*], Atsushi Funaki [b], Kiyotaka Arai [b]

[a] Department of Future Industry-oriented Basic Science and Materials, Toyota Technological Institute, Tempaku, Nagoya 468-8511, Japan
[b] Research and Development Division, Asahi Glass Co., Ltd., Yokohama, Kanagawa 221-8755, Japan

ARTICLE INFO

Article history:
Received 2 April 2008
Received in revised form 26 August 2008
Accepted 6 September 2008
Available online 20 September 2008

Keywords:
Ethylene–tetrafluoroethylene copolymer
Phase transition
X-ray diffraction

ABSTRACT

Phase transitional behavior has been investigated for a series of ethylene (E) and tetrafluoroethylene (TFE) two-component copolymers on the basis of the temperature dependent measurement of X-ray fiber diagrams taken for the uniaxially-oriented samples. The usage of such uniaxially-oriented samples has allowed us to clarify the structural changes more definitely than before. So far, the crystalline transition from the low-temperature phase to the high-temperature phase had been assumed to occur continuously, but the detailed analysis of the X-ray reflections at higher scattering angles revealed for the first time that the transition is of the thermodynamically-*discontinuous* first-order type between the monoclinic and the pseudohexagonal phases. This phase transition temperature shifted toward lower temperature side as the TFE content became higher. The analysis of the X-ray reflection profile allowed us to imagine that low-temperature shift of the transition point is considered to occur due to the easier thermal motion of the planar-zigzag chains around the chain axis because of looser packing of chains containing higher population of bulky CF_2CF_2 groups. From these experimental data a phase diagram has been built up to show the phase transition behaviors of a series of E/TFE copolymers in a systematic manner. The characteristic features of the structural disordering including *trans–gauche* conformational exchange have been also discussed on the basis of the data of polarized infrared and Raman spectra combined with the X-ray diffuse scatterings.

1. Introduction

Ethylene (E)–tetrafluoroethylene (TFE) copolymers [–(CH_2CH_2)–(CF_2CF_2)–] have been attracting many attentions industrially and scientifically because of their characteristic physical properties such as good mechanical properties, excellent chemical resistance, and high weatherability [1]. This copolymer is unique in such a point that the skeletal chains may be assumed approximately as a combination of the segments of polyethylene –$(CH_2CH_2)_n$–, polytetrafluoroethylene –$(CF_2CF_2)_n$–, and poly(vinylidene fluoride) –$(CH_2CF_2)_n$– in a random manner. Because of sensitive structural balance between E and TFE segments, the stability of molecular conformation is considered to change depending on the E/TFE relative content. This characteristic feature reflects on the phase transition behavior occurring in the heating and cooling processes as well as the crystal structure detected at room temperature [2–14]. In a previous paper, we reported a systematic change in crystal structure exhibited at room temperature for a series of E/TFE copolymers on the basis of X-ray fiber diagrams and polarized infrared and Raman spectra of uniaxially-oriented samples [14]. The copolymer takes a planar-zigzag chain conformation at room temperature although, strictly speaking, the repeating period changes slightly depending on the content [3,14,15]. This copolymer had been said to show the phase transition phenomenon between the orthorhombic-type unit cell and the pseudohexagonal cell by changing the temperature [3,4,6–10,12,13]. Since the TFE segments possess larger volume than the E segments, the chain packing becomes looser with increase in TFE content. It may be easily speculated that the phase transition temperature should be lower for a copolymer sample with higher TFE content. In fact, some papers had been published to show this phenomenon on the basis of X-ray diffraction data [6–10]. Unfortunately, however, the unoriented samples were mostly used in these studies for the X-ray diffraction measurements. So the separation of overlapping reflections is difficult to do, making the analysis more or less ambiguous. Besides only a few innermost reflections were mostly investigated for the discussion because the wider angle reflections were too weak to analyze in a quantitative manner for the

* Corresponding author. Tel.: +81 52 809 1790; fax: +81 52 809 1793.
E-mail address: ktashiro@toyota-ti.ac.jp (K. Tashiro).

0032-3861/$ – see front matter © 2008 Elsevier Ltd. All rights reserved.
doi:10.1016/j.polymer.2008.09.010

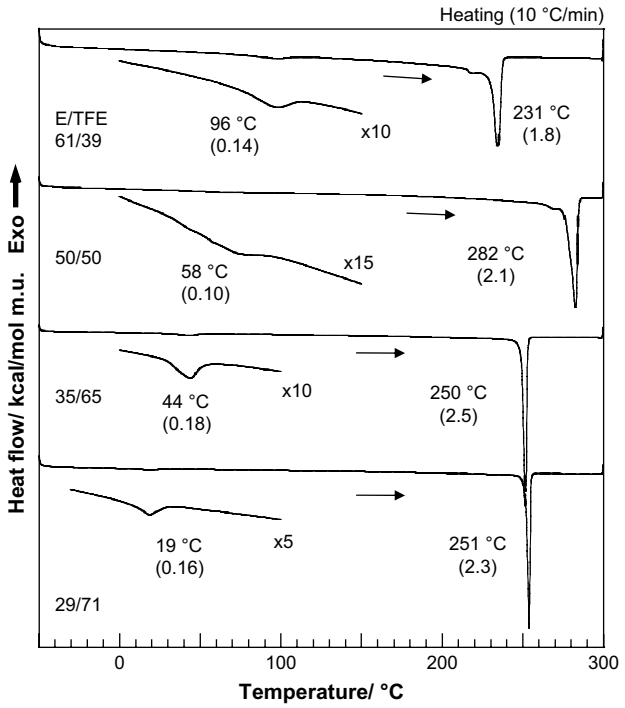

Fig. 1. DSC thermograms measured for a series of uniaxially-oriented E/TFE copolymer samples at the heating rate of 10 °C/min. The figures in parentheses are enthalpy changes in kcal/mol monomeric unit at phase transition or melting point.

unoriented samples. As will be reported here, utilization of uniaxially-oriented samples makes it possible to trace the change in the reflection profile more clearly and in a wider diffraction angle region. The observation of higher-angle reflections has lead us to the new and crystallographically important finding about the thermodynamic transition mode: the transition had been believed to be apparently continuous second-order type but the higher-angle data revealed for the first time that it should be assigned to the first-order type occurring in a *discontinuous* mode. Beside, we have noticed that the orthorhombic-type unit cell, which was proposed for the E/TFE copolymer of 50/50 E/TFE content [3], is not reasonable but should be of a *monoclinic* type judging from the characteristic reflections observed for a series of this copolymer.

Another important point of our present report is about the monomer components in the copolymer sample. Although there had been several papers describing the phase transition behavior of E/TFE copolymer sample with ''50/50 molar content'', for example, the samples actually used were not the pure two-component systems but contained to some extent the third component such as hexafluoropropylene or perfluoropropylvinylether judging from the sample source. The third (and forth) monomer component was reported to affect sensitively the phase transition behavior [6,10,16]. Therefore we may not conclude easily that the transition characteristics reported so far can be applied to those of the truly two-component system without any doubt. The reason why we reported the crystal structure exhibited at room temperature for a series of uniaixially-oriented two-component E/TFE copolymers is based on such a serious situation [14]. The 2-dimensional X-ray diffraction pattern changes remarkably depending on the E/TFE content. Each member of this series shows the phase transition at individually characteristic transition temperature as described in

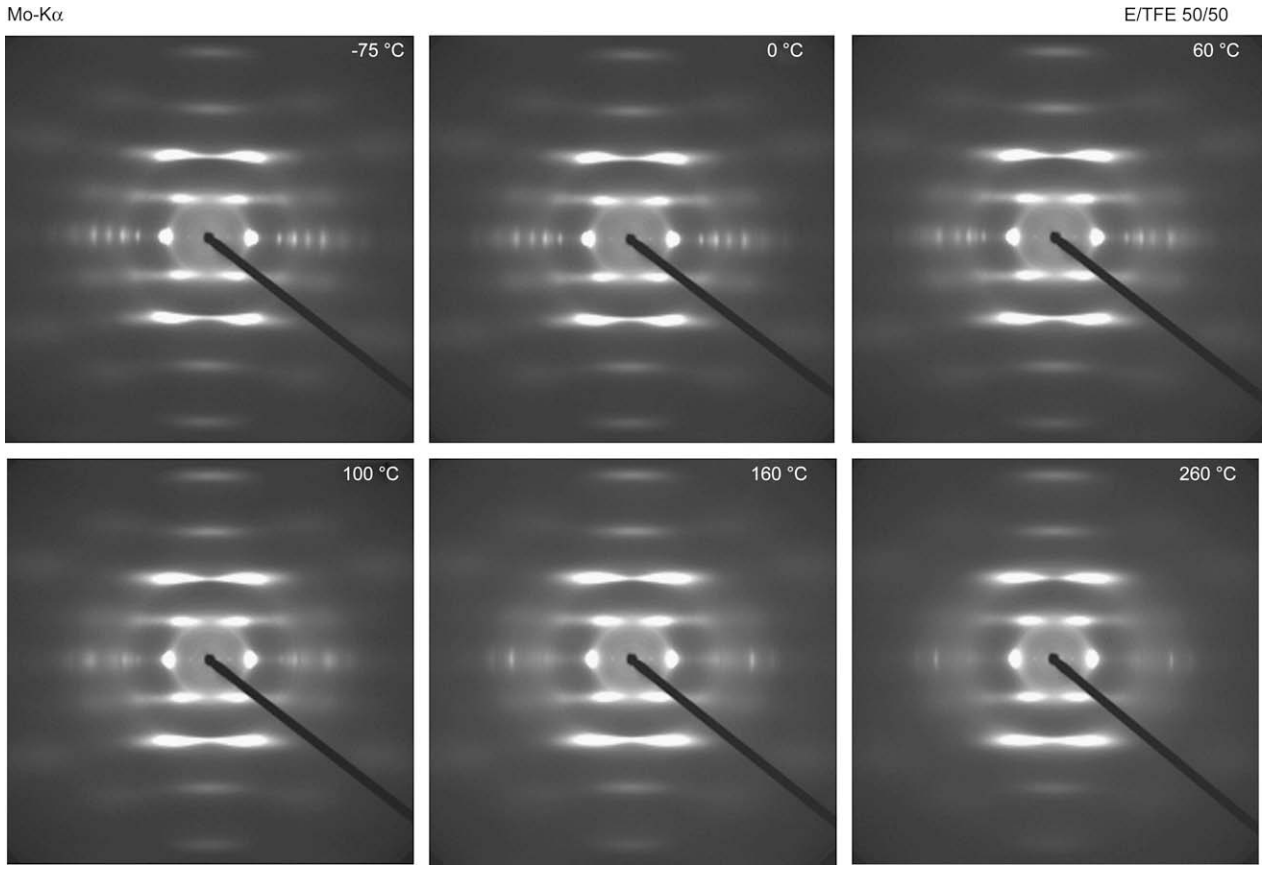

Fig. 2. X-ray fiber diagrams taken for uniaxially-oriented E/TFE 50/50 copolymer sample at various temperatures (heating process).

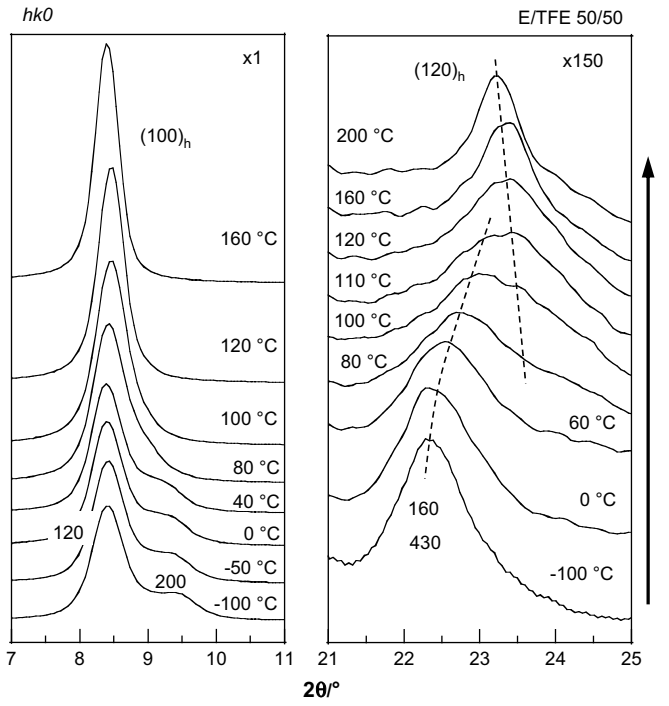

Fig. 3. Temperature dependence of the X-ray equatorial line profile of uniaxially-oriented E/TFE 50/50 copolymer sample obtained from Fig. 2. The Mo-Kα line was used as an incident X-ray beam.

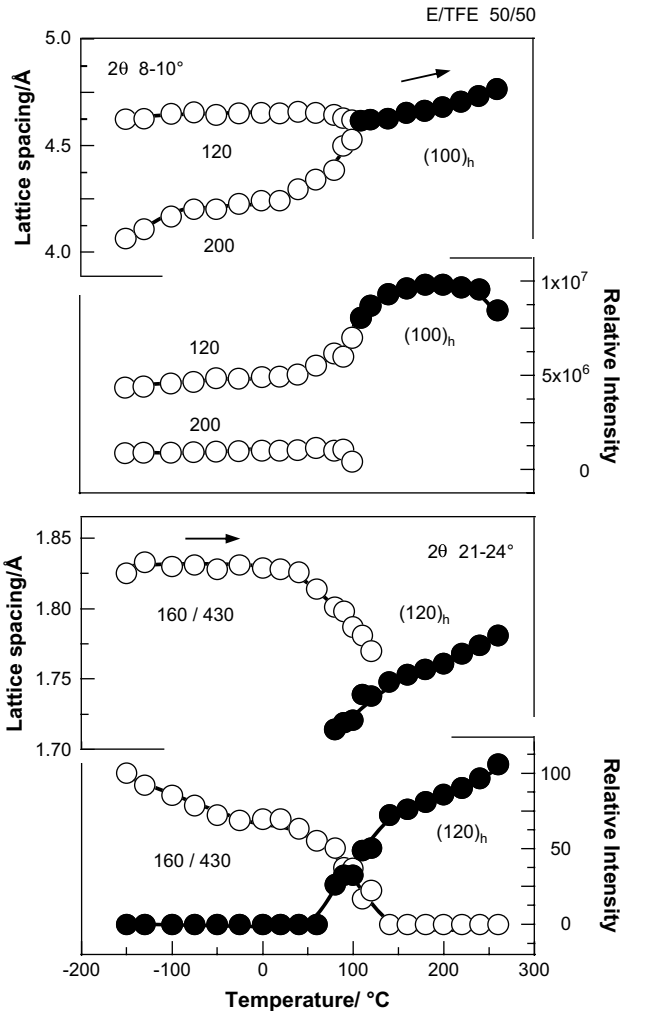

Fig. 4. Temperature dependence of the lattice spacing and diffraction intensity estimated for several X-ray equatorial reflections of uniaxially-oriented E/TFE 50/50 copolymer sample.

a later section. Therefore the third component makes such a systematic transition behavior more complicated and ambiguous. We need to use purely two-component systems of E and TFE monomeric units only.

In this way, in spite of the publication of relatively many papers, the accurate analysis of the phase transition behavior had not yet been made enough satisfactorily because the utilization of unoriented samples of more or less three-component system made the data analysis seriously ambiguous. From all the present situations mentioned above, we have investigated in detail the phase transition behavior of a series of uniaxially-oriented E/TFE copolymers on the basis of the temperature dependent measurement of X-ray fiber diagrams mainly. In some cases, we combined the X-ray diffraction data with the vibrational spectroscopic data for the concrete discussion on the conformational disordering in the phase transition. Based on the experimental data we have successfully deduced a kind of phase diagram which should show our new concept about this E/TFE copolymer system.

2. Experimental section

2.1. Samples

A series of E/TFE copolymers were synthesized by a radical polymerization reaction in the perfluoropentyl difluoromethane solution. The chemical composition was analyzed by the molten-state ^{19}F NMR measurement and the fluorine ultimate elementary analysis. The monomer contents of these copolymers were as follows: E/TFE = 61/39, 50/50, 35/65, and 29/71 mol%.

The samples were molten and quenched into ice-water bath to produce the low-crystalline materials, which were stretched about three times the original length at about 100 °C and then annealed at about 20 °C below the melting temperatures for 3 h under tension. The thus-prepared uniaxially-oriented samples with ca. 0.3 mm thickness were supplied to the X-ray diffraction and Raman spectral measurements. The oriented thin films of ca. 20 μm were used for the infrared spectral measurements.

2.2. Measurements

The X-ray fiber diagrams were measured using a MAC Science DIP1000 X-ray diffraction system with a graphite-monochromatized Mo-Kα line ($\lambda = 0.71073$ Å) as an incident X-ray beam. An imaging plate was used as the 2-dimensional detector. Temperature dependent measurements of the X-ray fiber diagrams were performed by blowing nitrogen gas onto the sample set on a goniometer head using a cryostat CryoMini Coldhead and a Rigaku temperature controller in the range of −150 to +260 °C. The temperature was monitored by a thermocouple attached directly to the sample. The temperature fluctuation was about ±1.0 °C. The DSC thermograms were obtained by DSC Q1000 (TA instruments, USA) in the temperature range of −50 to +300 °C at the heating rate 10 °C/min.

The Raman spectra were measured for the uniaxially-oriented samples at the various temperatures using a home-made heater. The spectra were measured using a JASCO NRS-2100 laser Raman spectrophotometer at the back-scattering geometry with a laser beam of 532 nm wavelength. The resolution power was 2 cm^{-1}. The polarized infrared spectra were measured at various temperatures

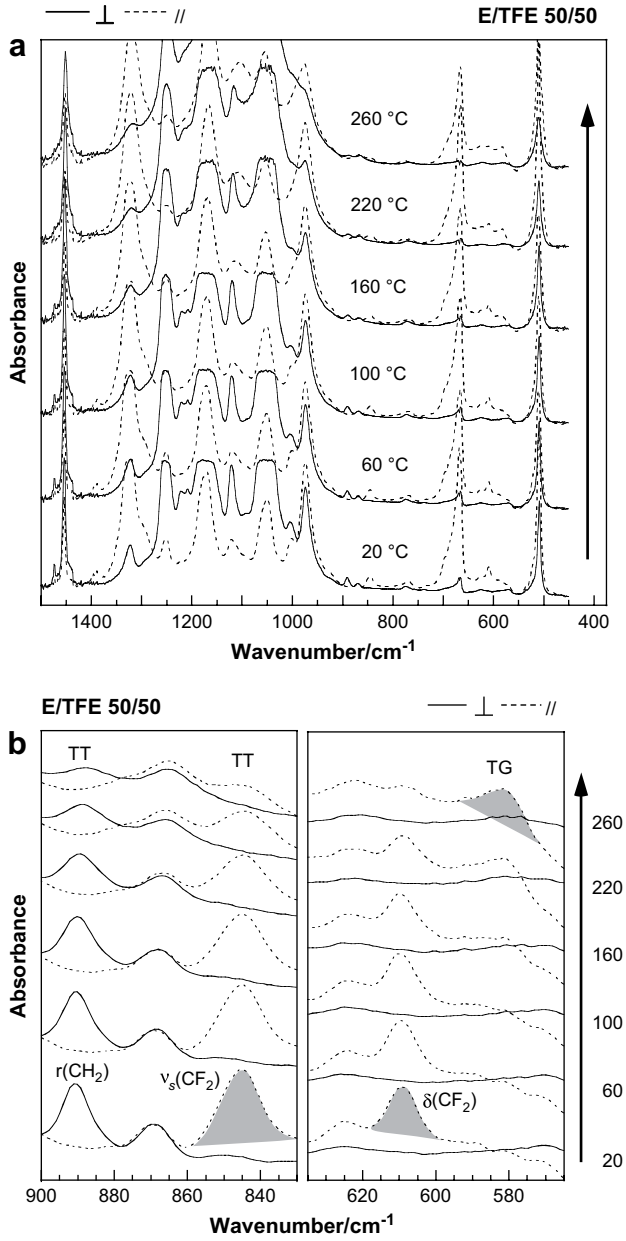

Fig. 5. Temperature dependence of the polarized infrared spectra measured for the uniaxially-oriented E/TFE 50/50 copolymer sample in the region of (a) 1500–450 and (b) 900–830 and 635–565 cm^{-1}. The solid and broken lines represent the spectra taken with the electric vector of the incident infrared beam perpendicular and parallel to the oriented direction, respectively.

with a Varian FTS-7000 Fourier-transform infrared spectrometer equipped with a wire-grid polarizer. The resolution power was 2 cm^{-1}.

3. Results and discussion

3.1. Phase transitional behaviors

Fig. 1 shows the DSC thermograms measured for a series of uniaxially-oriented E/TFE samples in the heating process. The peak temperatures and enthalpy changes were estimated for the endothermic peaks detected in these curves. The quite small endothermic peaks in the relatively low-temperature region correspond to the phase transitions although the details of structural changes are not known from the DSC data only. The sharp peak located at around 230–280 °C corresponds to the melting point [2,7,17]. The systematic discussion about these data will be made in a later section.

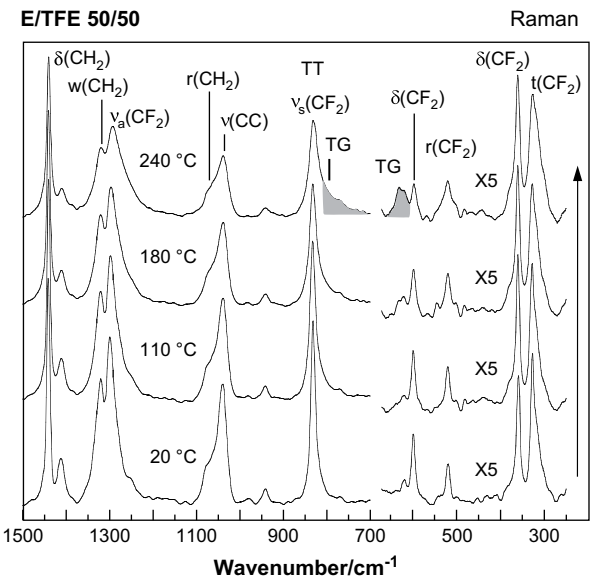

Fig. 6. Temperature dependence of the Raman spectra measured for the uniaxially-oriented E/TFE 50/50 copolymer sample.

3.1.1. E/TFE 50/50 copolymer

Fig. 2 shows the temperature dependence of X-ray fiber diagram taken for the uniaxially-oriented E/TFE 50/50 copolymer sample. The molecular chain takes the planar-zigzag conformation as known from the fiber period 5.1 Å estimated from the interlayer spacings [3,4,14,15]. The fiber diagram is as a whole diffuse: the diffuse scatterings can be detected for all the layer lines, indicating a disorder in relative height of the adjacent zigzag chains. Fig. 3 shows the equatorial line profile obtained from Fig. 2. The innermost reflections at $2\theta = 8.2°$ and 9.3° (Mo-Kα) suggest the presence of rectangular unit cell even at low temperature as reported in Refs. [4,5]. These reflections are indexed as 120 and 200 on the basis of

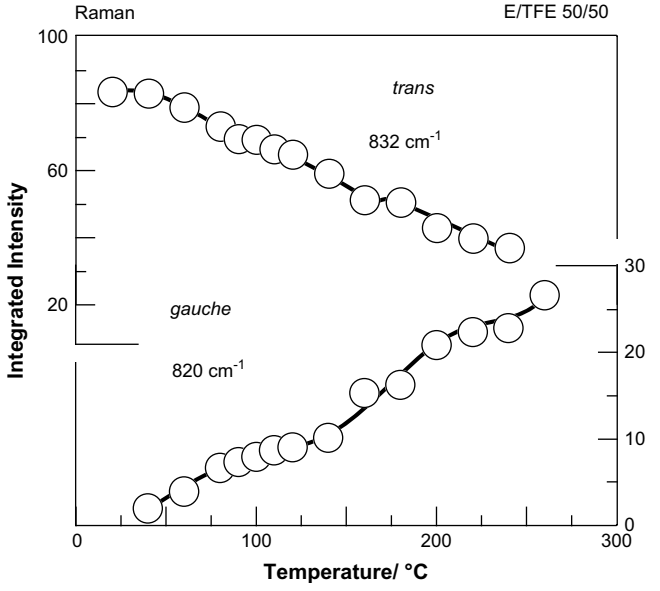

Fig. 7. Temperature dependence of the Raman intensity of *trans* (832 cm^{-1}) and *gauche* (820 cm^{-1}) bands estimated from Fig. 6.

apparently rectangular unit cell $a = 8.53$ Å, $b = 11.72$ Å, and c (fiber axis) $= 5.15$ Å. These two reflections approach each other apparently continuously with increasing temperature and merge into one at around 100 °C. However, when we focus on the higher-angle region around $2\theta = 22°$, the reflection (160 and 430) is found to coexist with a newly appearing reflection at about $2\theta = 23°$ when the temperature is in the range of broad endothermic peak of 50–100 °C (Fig. 1). As the temperature increases furthermore, the higher-angle reflection increases in intensity and the original lower-angle reflection disappears completely. Therefore, we may say that the transition is not continuous but it occurs *discontinuously* in the thermodynamical 1st-order mode between the apparently orthorhombic-type cell and the pseudohexagonal cell as seen in Fig. 4, although many researchers had believed the continuous 2nd-order-type transition from the innermost reflections only.

As already reported, the *trans*-zigzag chains at lower temperature experience the conformational disorder above the transition point through the partially-occurring *trans–gauche* exchange [12,18,19]. We performed the temperature dependent measurement of infrared and Raman spectra for uniaxially-oriented E/TFE 50/50 copolymer sample. For example, Figs. 5 and 6 show, respectively, the polarized infrared spectra and Raman spectra taken at the various temperatures in the heating process. The bands at 581 cm^{-1} increased in intensity as the temperature was increased and the bands at 890, 845 cm^{-1}, etc. assigned to the *trans*-zigzag bands decreased in intensity. The similar observation can be made also in the Raman spectra as shown in Fig. 7 for the intensity exchange between the *trans* (832 cm^{-1}) and *gauche* (820 cm^{-1}) bands. Fig. 8 shows the temperature dependence of the absorbance estimated for these several infrared bands. In this figure a half-width of 1454 cm^{-1} band is also plotted against temperature, which reflects the activity of thermally-activated rotational motion of the molecular chains in a crystal lattice. From Fig. 7, we can

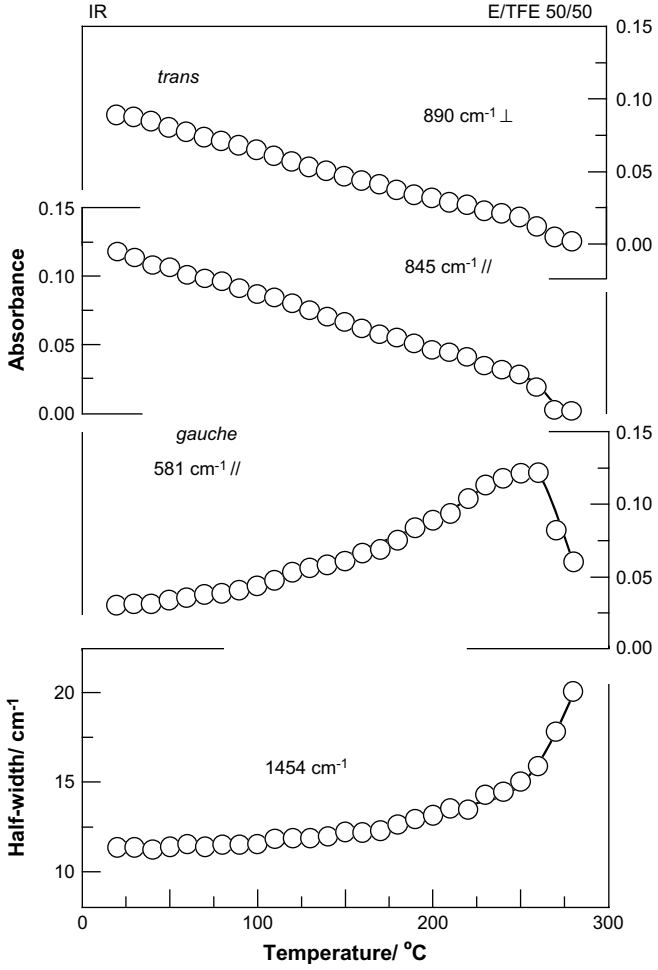

Fig. 8. Temperature dependence of the infrared absorbance of *trans* and *gauche* and the half-width of 1454 cm^{-1} band estimated from Fig. 5.

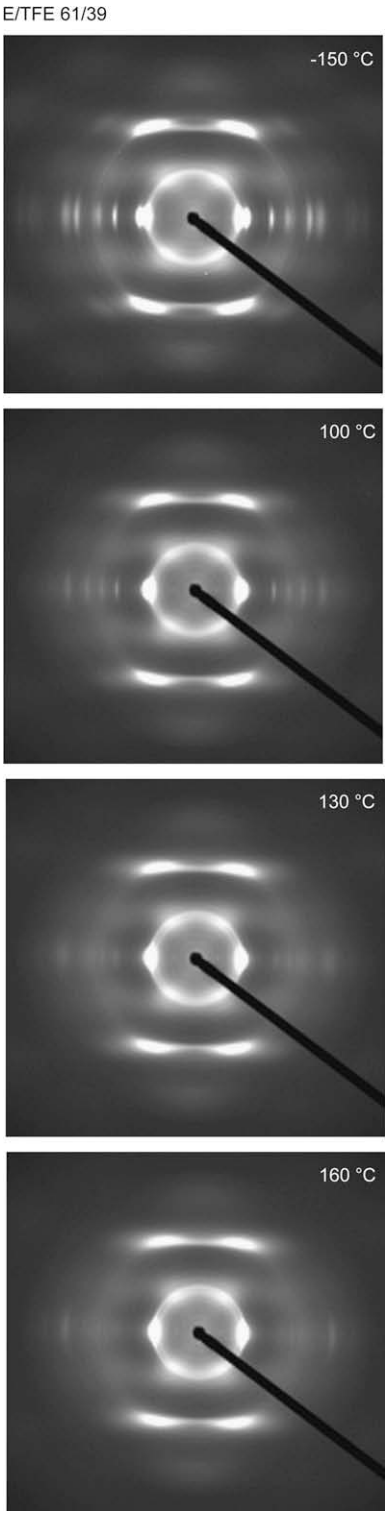

Fig. 9. Temperature dependence of X-ray fiber diagram taken for uniaxially-oriented E/TFE 61/39 copolymer sample (heating process).

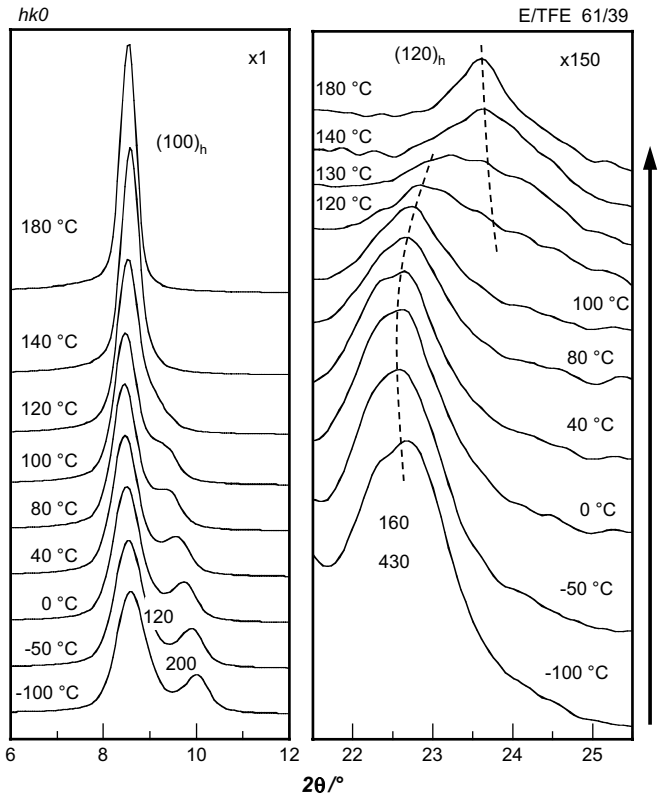

Fig. 10. Temperature dependence of the X-ray equatorial line profile of uniaxially-oriented E/TFE 61/39 copolymer sample obtained from Fig. 9.

evaluate the conformational energy difference between the *trans* and *gauche* forms by performing the logarithmic plot of relative intensity of the *trans* (832 cm^{-1}) and *gauche* (820 cm^{-1}) bands under the assumption that the relative contents of *trans* and *gauche* forms are in proportion to the Boltzmann distributions: $X_i \propto \exp(-E_i/kT)$ where X_i is the relative fraction of i conformer, E_i is the corresponding conformation energy, and k is the Boltzmann constant. The energy difference $\Delta E = E_{gauche} - E_{trans}$ was obtained as +3.0 kcal/mol monomeric unit. This indicates that the *trans* form is appreciably more stable than the *gauche* conformation. By referring to the energy calculations [19,20], the conformational barrier of the CC torsional angle around CH_2–CF_2 bonds is lower than those of CH_2–CH_2 and CF_2–CF_2 bonds. Therefore we may speculate that the conformational disordering between the

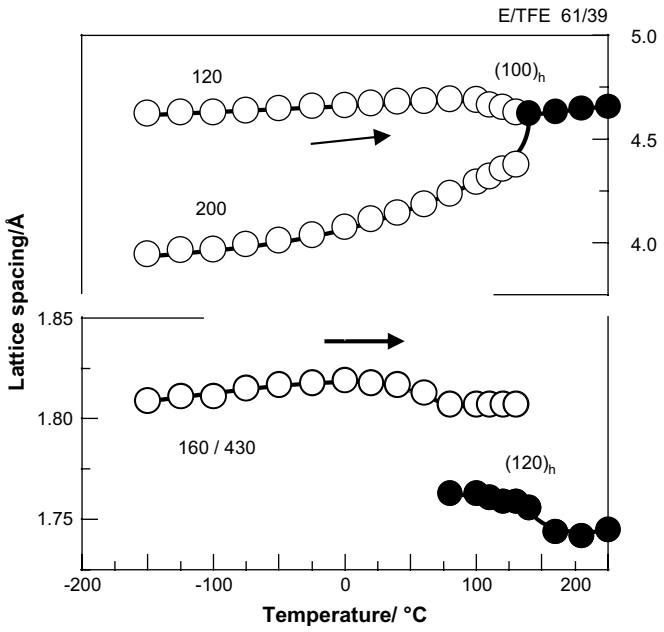

Fig. 11. Temperature dependence of the lattice spacings of uniaxially-oriented E/TFE 61/39 copolymer sample estimated from Fig. 10.

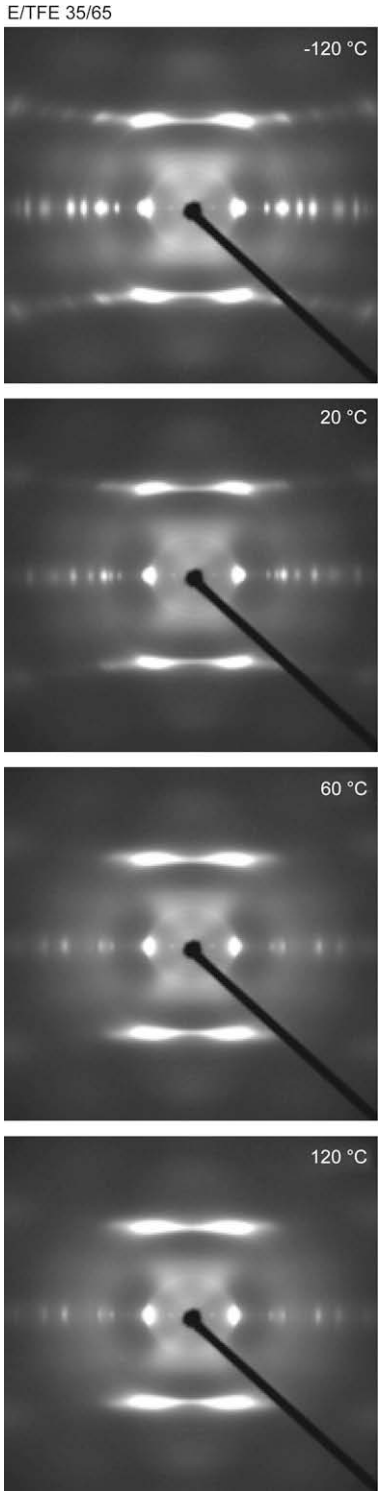

Fig. 12. X-ray fiber diagrams taken for uniaxially-oriented E/TFE 35/65 sample at various temperatures (heating process).

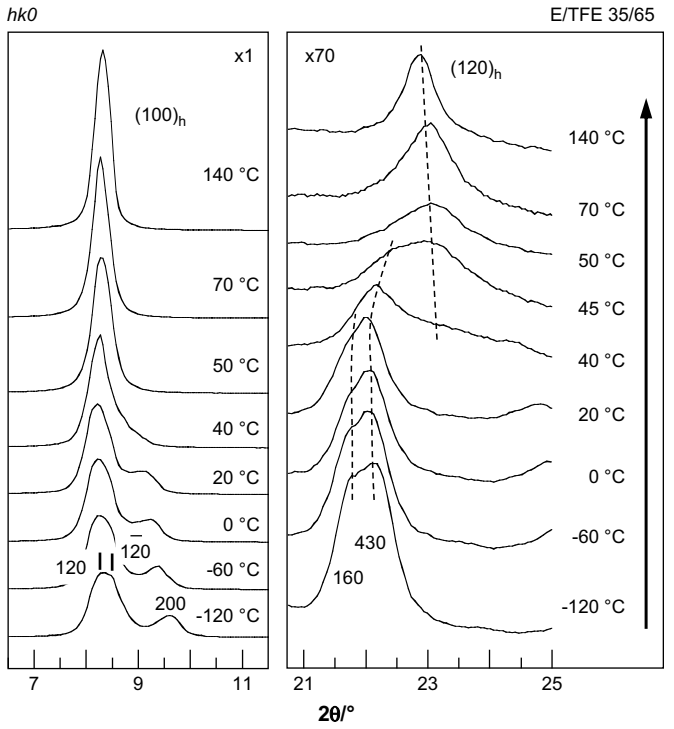

Fig. 13. Temperature dependence of the X-ray equatorial line profile of uniaxially-oriented E/TFE 35/65 sample obtained from Fig. 12.

low- and high-temperature phases occurs through the *trans–gauche* conformational motion around the CH_2–CF_2 linkages. Besides, the structural changes should be associated with the rotational motion of the whole chains as speculated from the remarkable change in the half-width of 1454 cm^{-1} band (Fig. 8). The similar treatment can be made also for the X-ray diffraction data. From Fig. 4 we plot the logarithm of relative intensity ratio of the reflections intrinsic to the low- and high-temperature phases against temperature, leading to $\Delta E = 12.0$ kcal/mol. Since the four chains are included in the unit cell [3], the energy difference of the low- and high-temperature phases is about 3.0 kcal/mol monomeric unit, which is consistent with the result obtained by the vibrational spectroscopy.

3.1.2. E/TFE 61/39 copolymer

In Fig. 9 are shown the X-ray fiber diagrams of the uniaxially-oriented E/TFE 61/39 sample taken at various temperatures. Compared with the 50/50 copolymer, the 1st and 3rd layer lines become more diffuse because the contribution of planar-zigzag ethylene sequences of 2.55 Å period is increased gradually in the structure factors as already reported previously [14]. The temperature dependence of the equatorial line profile given in Fig. 10 shows the similar behavior to that of E/TFE 50/50 copolymer (Fig. 3). The unit cell parameters are determined to be $a = 8.33$ Å, $b = 12.00$ Å, c (fiber axis) $= 5.18$ Å, and $\gamma = 90°$ at -100 °C. The higher-angle reflections at about 22° (160 and 430) are weaker above the transition point of ca. 130 °C, and the newly appearing reflections coexist with them in the transition region. In Fig. 11 are plotted the lattice spacings evaluated from Fig. 10. The reflections observed above the phase transition temperature can be indexed based on the pseudohexagonal lattice of $a = b = 5.60$ Å and $\gamma = 120°$. In this way, the E/TFE 61/39 copolymer shows also the *discontinuous* first-order type phase transition between the apparently rectangular cell and the pseudohexagonal cell.

Table 1
Tentative unit cell parameters of uniaxially-oriented E/TFE samples at −100 °C

E/TFE	a/Å	b/Å	c (fiber axis)/Å	γ/°
61/39	8.33	12.00	5.18	90
50/50	8.53	11.72	5.15	90
35/65	8.81	12.51	5.14	93
29/71	8.89	12.30	5.13	93

3.1.3. E/TFE 35/65 copolymer

Fig. 12 shows the X-ray fiber diagrams of the oriented E/TFE 35/65 copolymer measured at the various temperatures. The first layer line detected between the equatorial and the bright 2nd layer lines becomes further weaker than the case of E/TFE 61/39 copolymer [14]. This comes from the coherent scattering from the randomly-arrayed E and TFE units along the molecular chain as the E/TFE content deviates from 50/50 ratio. The relatively long E sequences and TFE sequences with 2.55 Å periods are generated at some probabilities, resulting in weaker intensity of the original first layer reflections of E/TFE 50/50 copolymer [14]. As the temperature increases, the layer lines become more diffuse but keep the interlayer spacings corresponding to the planar-zigzag form even at 120 °C.

As shown in Fig. 13, the innermost equatorial reflection at $2\theta = 8.0°$ is apparently single at room temperature and might be indexed as 120. But it is found to consist of two components at −120 °C. Therefore, it is impossible to assume an orthorhombic unit cell but we need to reduce the symmetry to monoclinic. These two reflections are indexed as 120 and $1\bar{2}0$. The unit cell parameters are $a = 8.81$ Å, $b = 12.51$ Å, c (fiber axis) $= 5.14$ Å, and $\gamma = 93.0°$ as shown in Table 1. The three reflections (120, $1\bar{2}0$, and 200) in the 2θ region of 8–10° merge into one at higher temperature. On the way of transition, the higher-angle peaks at $2\theta = 20$–26° coexist with the newly appearing reflections, indicating an occurrence of the *discontinuous* first-order phase transition between monoclinic

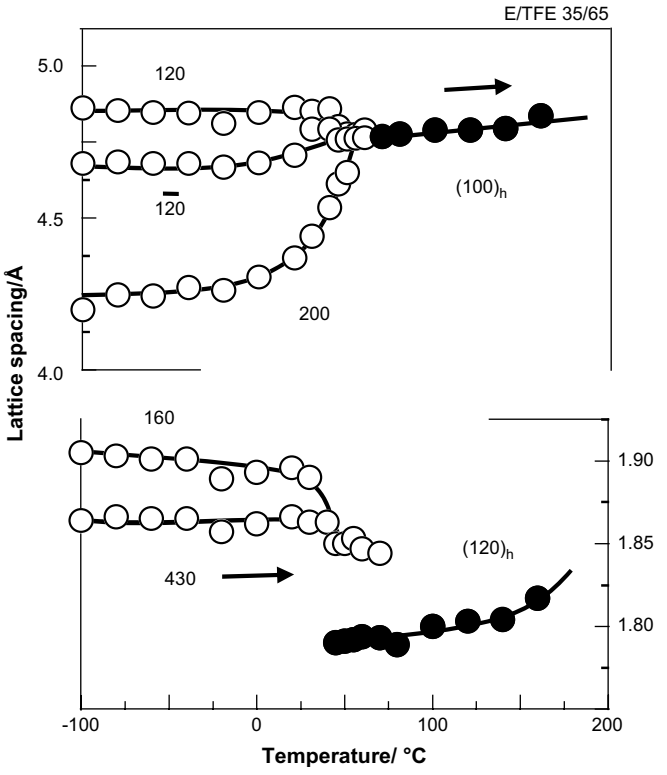

Fig. 14. Temperature dependence of the lattice spacings estimated for several X-ray equatorial reflections of uniaxially-oriented E/TFE 35/65 copolymer sample.

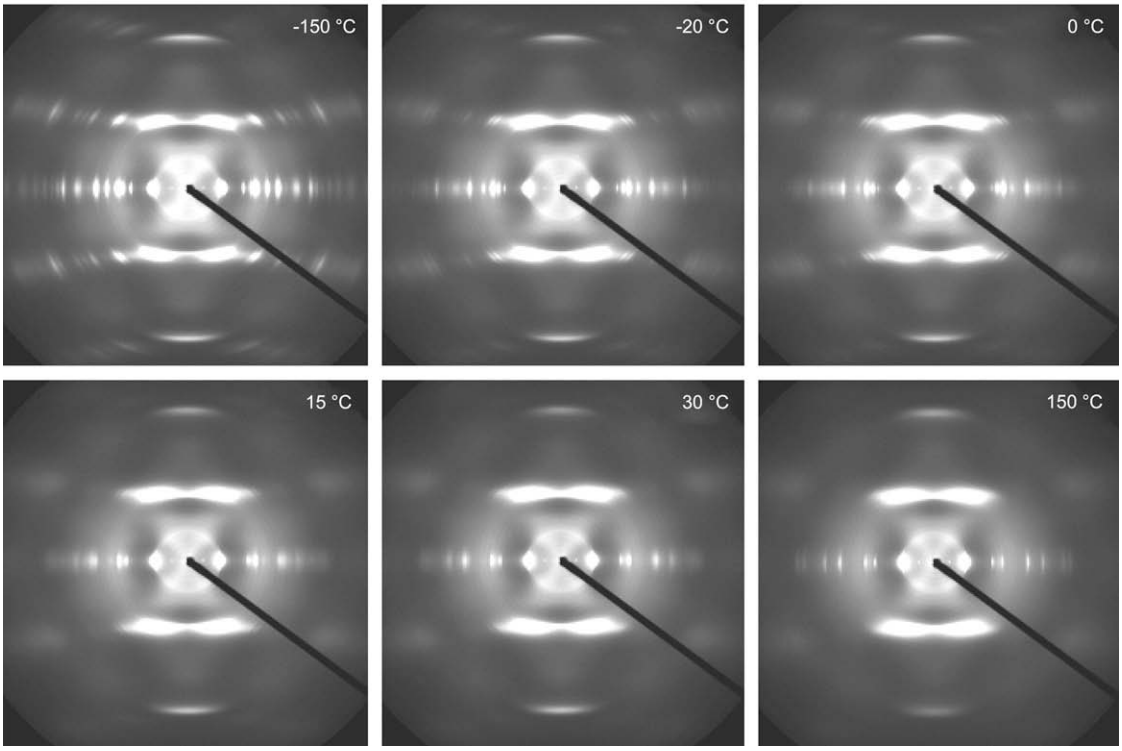

Fig. 15. X-ray fiber diagrams taken for uniaxially-oriented E/TFE 29/71 copolymer sample at various temperatures (heating process).

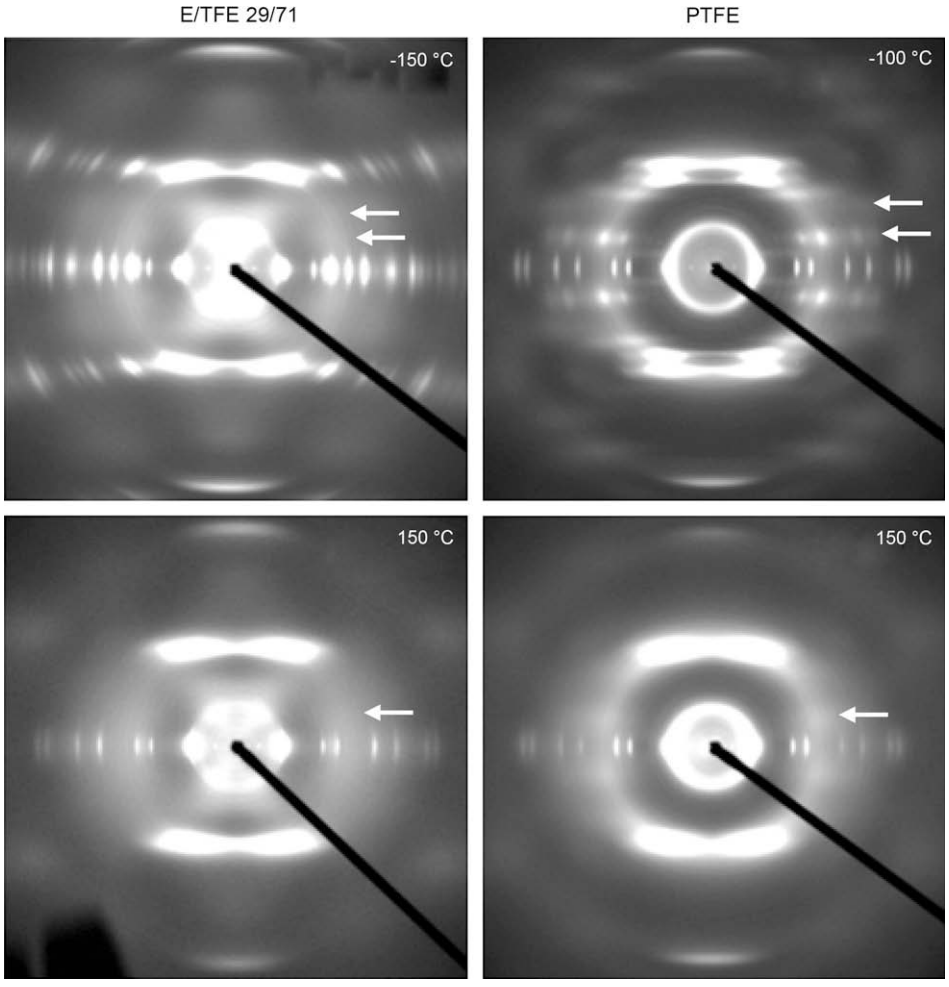

Fig. 16. Comparison of X-ray fiber diagram between uniaxially-oriented E/TFE 29/71 copolymer and polytetrafluoroethylene measured at low and high temperatures.

lattice and pseudohexagonal lattice as plotted in Fig. 14. Above the transition point they change *discontinuously* to the pseudohexagonal lattice.

3.1.4. E/TFE 29/71 copolymer

Fig. 15 shows the X-ray fiber diagrams taken for the E/TFE 29/71 copolymer at the various temperatures. The layer line reflections are sharp and intense at −150 °C. As the temperature increases, these reflections become more diffuse [13]. When we investigate the X-ray fiber diagram taken at the various temperatures, we can notice the existence of diffuse layer line in between the clear first layer and equatorial lines. As compared in Fig. 16 these diffuse layer lines (white arrows) are similar to those observed for polytetrafluoroethylene sample [21–23], and so they are considered to reflect the partial presence of helical sequential parts included in the skeletal chain of this copolymer, giving a shorter fiber period of 5.1 Å than the perfect zigzag form. Fig. 17 shows the temperature dependence of the equatorial line profile estimated from Fig. 15. The equatorial line becomes sharper with increasing temperature. The innermost reflections consist of two peaks at 8.2° and 8.4° (120 and $1\bar{2}0$) in addition to the weaker reflection at about 9.4° (200). We need again to apply the monoclinic unit cell instead of the orthorhombic cell (Table 1). With increasing temperature these three reflections merge into one above the room temperature as shown in Fig. 18(a). Above 0 °C, the higher-angle reflections at $2\theta \sim 20°$ decrease in intensity and the new reflection appears separately at 22.5° and increases in intensity (Fig. 18(b)). Therefore, this copolymer is considered to exhibit also the thermodynamic first-order transition between monoclinic and pseudohexagonal cells.

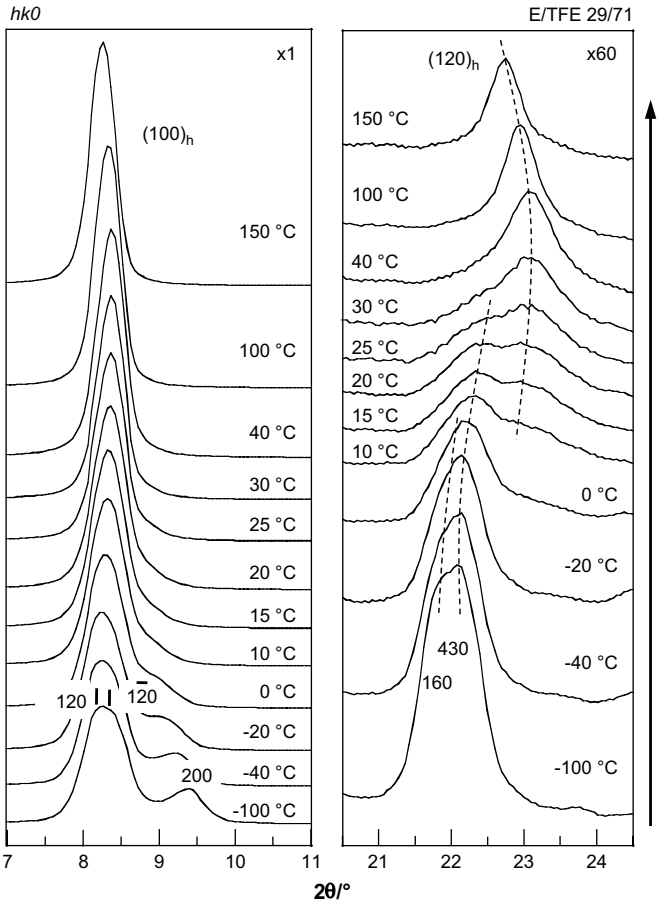

Fig. 17. Temperature dependence of the X-ray equatorial line profile of E/TFE 29/71 copolymer obtained from Fig. 15.

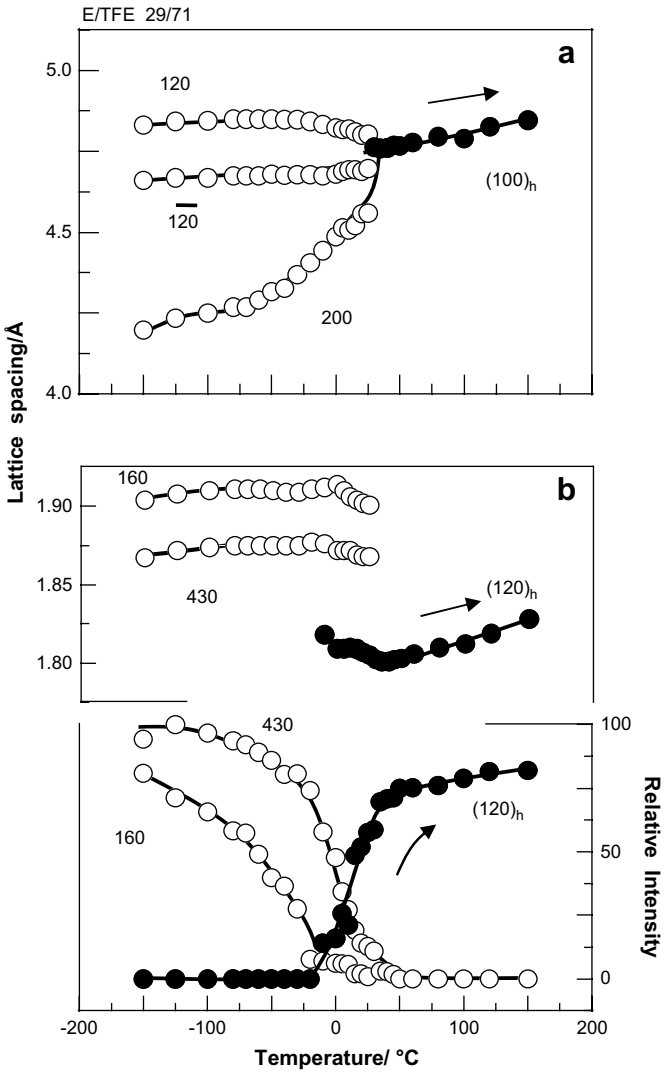

Fig. 18. Temperature dependence of (a) the lattice spacing evaluated from the X-ray innermost equatorial reflections and (b) the lattice spacing and diffraction intensity estimated for several X-ray equatorial reflections in the region $2\theta = 21–24°$ of uniaxially-oriented E/TFE 29/71 copolymer sample.

3.2. Phase diagram

When we see the lower-angle X-ray equatorial region ($2\theta = 8–10°$) as shown in Fig. 19(a), the transition occurs apparently continuously in the 2nd-order type for a series of E/TFE copolymers. However, observing the higher-angle region, e.g. $2\theta = 21–24°$ (Fig. 19(b)), all the copolymer samples treated here are found to exhibit the *discrete* first-order phase transition between the low-temperature monoclinic lattice and the high-temperature pseudohexagonal lattice.

On the basis of the X-ray diffraction and DSC data presented in this paper, we build up a phase diagram as shown in Fig. 20. The transition from low-temperature monoclinic to high-temperature pseudohexagonal phases occurs *discontinuously* and the phase transition temperature changes depending on the E/TFE content in a systematic manner. The vertical bars show the temperature region of the coexistence of the low- and high-temperature phases. The transition behavior may be classified into three groups. Group C for the members with high amount of TFE content shows the transition similar to PTFE in a relatively low-temperature region. The melting point is quite high when TFE content is close to PTFE.

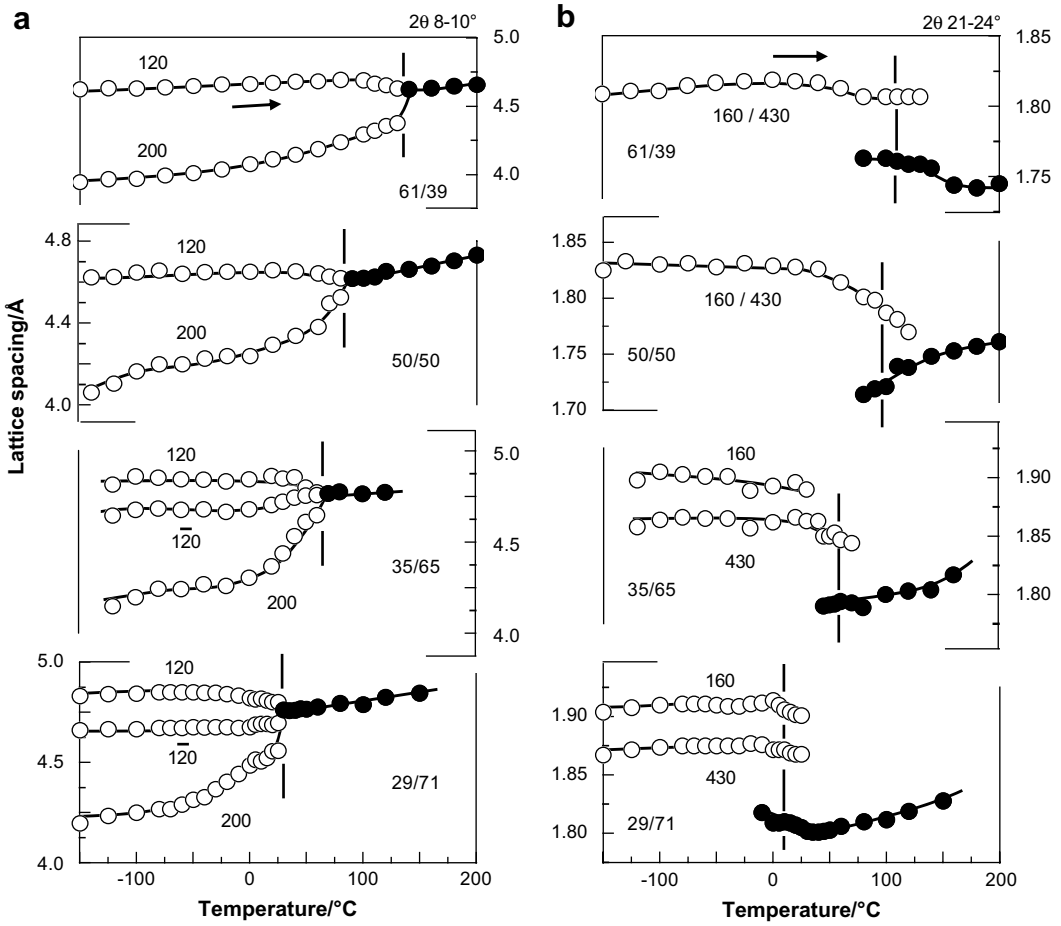

Fig. 19. Temperature dependence of the lattice spacings in the scattering angle regions of (a) $2\theta = 8–10^\circ$ and (b) $2\theta = 21–24^\circ$ compared for a series of E/TFE copolymers.

The transition of the group B is sensitive to the ethylene content as seen in the relatively sharp change of transition temperature in this region. In the group A, the transition point is closer to melting point by increasing E content. As known well E/TFE copolymer with 100% E content or polyethylene shows the transition from pseudohexagonal to melt at almost the melting point [24–27].

3.3. Characteristic features of structural disordering

As for the structural change, the molecular conformation is essentially the planar-zigzag form and it is disordered more or less above the transition temperature due to the *trans–gauche* conformational exchange as discussed for E/TFE 50/50 copolymer sample based on the infrared and Raman spectral data [12,18,19]. But the degree of this conformational exchange is not very high and different from the cases of vinylidene fluoride–trifluoroethylene (VDF–TrFE) copolymers [28,29] and vinylidene fluoride–tetrafluoroethylene (VDF–TFE) copolymers [28,30–32]. Based on the molecular dynamics simulation, we have found that the E/TFE copolymers are overwhelmingly stable as the *trans*-zigzag form and the conformational disorder occurs at lower probability [19]. In other words, the order-to-disorder transition is considered to occur mainly through the rotational motion of essentially *trans*-zigzag chains with some conformational disordering.

Fig. 21 shows the temperature dependence of relative intensity of the Bragg reflections and the diffuse scattering on the 2nd layer line. For example, in the case of E/TFE 50/50 copolymer, the Bragg reflection (122) starts to decrease in intensity around 60 °C, corresponding to the small endothermic peak in the DSC thermogram.

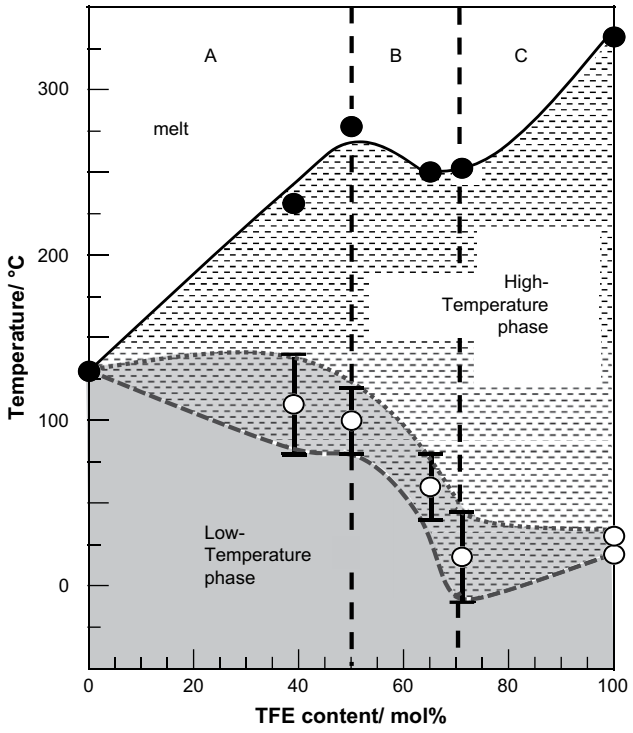

Fig. 20. Phase diagram of E/TFE copolymer built up on the basis of DSC and X-ray fiber diagram data obtained in the heating process. Filled and open circles represent the melting and transition temperatures, respectively.

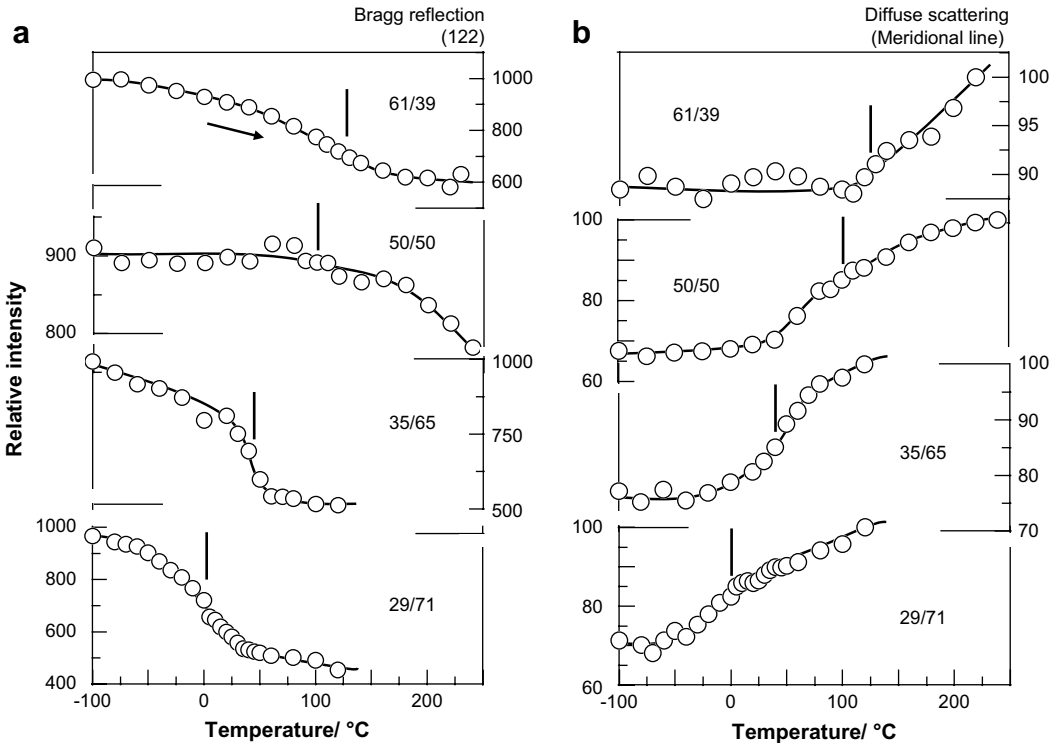

Fig. 21. Temperature dependence of X-ray scattering intensity estimated for (a) Bragg reflection (122) and (b) diffuse scattering in the meridional direction on the 2nd layer line.

The diffuse scattering increases in the same temperature region. The similar observation can be made for all the E/TFE copolymers treated in this paper. The intensity change occurs in the phase transition temperature region. The diffuse scattering along the horizontal line is considered to come from the disorder in relative height of the neighboring zigzag chains in the unit cell. We might speculate the structural disordering in the phase transition of E/TFE copolymer as follows.

At low temperature, the *trans*-zigzag chains are packed in the monoclinic lattice. As the temperature approaches the phase transition region, the rotational (or librational) motion of the zigzag chains starts to occur and some conformational exchanges occur also between the *trans* and the *gauche* forms. These two types of motion may be correlated with each other as indicated by the molecular dynamics calculation [19]. The chain packing becomes of a hexagonal type. At the same time, the relative height of the neighboring chains is shifted randomly by translational motion. As a result, the correlation between the neighboring chains becomes weaker, reflecting on the increase of X-ray diffuse scattering intensity and the decrease of Bragg reflection intensity as seen in Fig. 21. Judging from the similarity in the temperature dependence of X-ray diffraction, IR/Raman, and DSC thermal data, this type of structural disordering is considered to occur commonly for all the members of E/TFE copolymer although the transition temperature and the melting temperature are different depending on the E/TFE content as already pointed out in Figs. 1, 19, and 20. Fig. 22 illustrates the structural changes in a schematic manner.

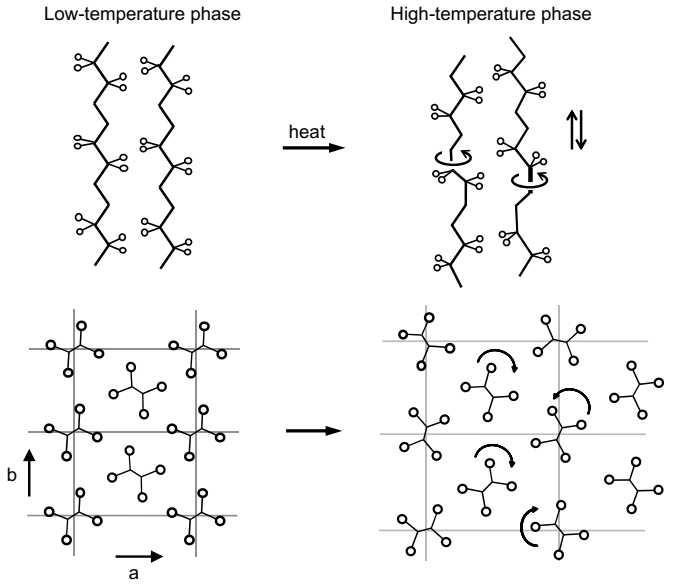

Fig. 22. A schematic illustration of structural transition between the low- and high-temperature phases of E/TFE copolymer.

4. Conclusions

In the present paper we have measured the 2-dimensional X-ray fiber diagrams of a series of two-component E/TFE copolymers as a function of temperature and built up a phase diagram successfully to clarify the transition scheme of this copolymer. As known from the remarkable changes in the X-ray equatorial line profile and the diffuse scattering intensity, the transition occurs between the monoclinic and pseudohexagonal lattice attendant with the rotational and translational disordering of the *trans*-zigzag chains with the partial conformational exchange between *trans* and *gauche* forms. This conformational disordering was supported reasonably by the temperature-dependent measurements of infrared and Raman spectra [12,18,19]. The phase transitional behavior of E/TFE copolymer is appreciably different from that of VDF/TrFE copolymer in such a point that the chain conformation is overwhelmingly stable in the *trans*-zigzag form and the *trans*-to-*gauche*

conformational change occurs at relatively low frequency in the E/TFE cases.

As for the crystal structure of the low-temperature phase, the previously-proposed orthorhombic cell is inconsistent with the X-ray diffraction data presented here. Rather the crystal lattice of monoclinic type is more plausible as known from the successful indexing of all the observed reflections including the well-separated equatorial line reflections such as 120 and $1\bar{2}0$ and so on. The details of the crystal structure analysis will be reported in a separate paper.

The structural changes revealed in the present paper have intimate relation with the temperature dependence of mechanical property as known from the detailed measurements of the dynamic viscoelastic property [33,34]. The Young's modulus decreases remarkably in the order-to-disorder phase transition temperature region because of the conformational disordering of the molecular chains as well as the rotational/translational motion of these chains.

Acknowledgement

This work was financially supported by MEXT "Collaboration with Local Communities" Project (2005–2009).

References

[1] Drobny J. Rapra Rev Rep 2006;16:184.
[2] Modena M, Garbuglio C, Ragazzini M. J Polym Sci Polym Lett Ed 1972;10:153–6.
[3] Tanigami T, Yamaura K, Matsuzawa S, Ishikawa M, Mizoguchi K, Miyasaka K. Polymer 1986;27:999–1006.
[4] Tanigami T, Yamaura K, Matsuzawa S, Ishikawa M, Mizoguchi K, Miyasaka K. Polymer 1986;27:1521–8.
[5] Scheerer K, Wilke W. Colloid Polym Sci 1987;265:206–9.
[6] Pieper T, Heise B, Wilke W. Polymer 1989;30:1768–75.
[7] Iuliano M, De Rosa C, Guerra G, Petraccone V, Corradini P. Makromol Chem 1989;190:827–35.
[8] Guerra G, De Rosa C, Iuliano M, Petraccone V, Corradini P, Ajroldi G. Macromol Chem Phys 1993;194:389–96.
[9] Radice S, Del Fanti N, Castiglioni C, Del Zoppo M, Zerbi G. Macromolecules 1994;27:2194–9.
[10] D'Aniello C, De Rosa C, Guerra G, Petraccone V, Corradini P, Ajroldi G. Polymer 1995;36:967–73.
[11] Radice S, Del Fanti N, Zerbi G. Polymer 1997;38:2753–8.
[12] Phongtamrug S, Tashiro K, Funaki A, Arai K, Aida S. Macromol Symp 2006;242:268–73.
[13] Phongtamrug S, Tashiro K, Funaki A, Arai K, Aida S. Polym Prepr Jpn 2007;56:717.
[14] Phongtamrug S, Tashiro K, Funaki A, Arai K, Aida S. Polymer 2008; 49:561–9.
[15] Wilson FC, Starkweather Jr HW. J Polym Sci Part A Polym Chem 2 1973; 11:919–27.
[16] Funaki A, Arai K, Aida S, Phongtamrug S, Tashiro K. Polym Prepr Jpn 2007;56:3807.
[17] Pucciariello R. J Appl Polym Sci 1996;59:1227–35.
[18] Tashiro K, Kobayashi M. Polym Prepr Jpn 1987;36:2339–41.
[19] Phongtamrug S, Tashiro K, Arai K, Funaki A. Polym Prepr Jpn 2007;56:3917–8.
[20] Farmer BL, Lando JB. J Macromol Sci Phys 1975;B11:89–119.
[21] Bunn CW, Howells ER. Nature 1954;174:549–51.
[22] Sperati CA, Starkweather Jr HW. Adv Polym Sci 1961;2:465–95.
[23] Clark ES, Muus LT. Z Kristallogr 1962;117:119–27.
[24] Clough SB. J Polym Sci Polym Lett Ed 1970;8:519–23.
[25] Pennings AJ, Zwijnenburg A. J Polym Sci Polym Phys Ed 1979;17:1011–32.
[26] Tashiro K, Sasaki S, Kobayashi M. Macromolecules 1996;29:7460–9.
[27] Rein DM, Shavit L, Khalfin RL, Cohen Y, Terry A, Rastogi S. J Polym Sci Part B Polym Phys 2004;42:53–9.
[28] Tashiro K. Crystal structure and phase transition of PVDF and related copolymers. In: Nalwa HS, editor. Ferroelectric polymers: chemistry, physics, and technology. Marcel Dekker Inc; 1995. p. 63–182.
[29] Lovinger AJ. Macromolecules 1983;16:1529–34.
[30] Green J, Rabolt JF. Macromolecules 1987;20:456–7.
[31] Tashiro K, Kaito H, Kobayashi M. Polymer 1992;33:2915–28.
[32] Tashiro K, Kaito H, Kobayashi M. Polymer 1992;33:2929–33.
[33] Starkweather Jr HW. J Polym Sci Polym Phys Ed 1973;11:587–93.
[34] Arai K, Funaki A, Aida S, Phongtamrug S, Tashiro K. Polym Prepr Jpn 2008;57:701.